Microstructure and mechanical properties of a hot-extruded Al-based composite reinforced with core–shell-structured Ti/Al$_3$Ti

Li Zhang[1,2], *Bao-lin Wu*[1,2], *and Yu-lin Liu*[1,2]

1) School of Materials Science and Engineering, Shenyang Aerospace University, Shenyang 110136, China

2) Liaoning Key Laboratory of Aviation Light Alloy and Processing Technology, Shenyang Aerospace University, Shenyang 110136, China

Abstract: An Al-based composite reinforced with core–shell-structured Ti/Al$_3$Ti was fabricated through a powder metallurgy route followed by hot extrusion and was found to exhibit promising mechanical properties. The ultimate tensile strength and elongation of the composite sintered at 620°C for 5 h and extruded at a mass ratio of 12.75:1 reached 304 MPa and 14%, respectively, and its compressive deformation reached 60%. The promising mechanical properties are due to the core–shell-structured reinforcement, which is mainly composed of Al$_3$Ti and Ti and is bonded strongly with the Al matrix, and to the reduced crack sensitivity of Al$_3$Ti. The refined grains after hot extrusion also contribute to the mechanical properties of this composite. The mechanical properties might be further improved through regulating the relative thickness of Al–Ti intermetallics and Ti metal layers by adjusting the sintering time and the subsequent extrusion process.

Keywords: microstructure; aluminum-based composites; Ti/Al$_3$Ti; reinforcements; mechanical properties

1. Introduction

Particulate-reinforced aluminum matrix composites (PRAMCs) have potential applications in the aviation, aerospace, and automotive fields because of their outstanding mechanical properties, which include high specific strength, high specific modulus, high hardness, and low thermal expansion [1–2]. PRAMCs with ceramic particles such as SiC, Al$_2$O$_3$, and B$_4$C as the reinforcement material have been well developed. However, brittle layers always form between particles and the Al matrix because of chemical reactions that usually result in weakening of the interfacial bonding [3]. Reducing the harmful effect of this brittleness on the properties of such composites is an important research topic.

If a casting method is used, the formation of brittle layers should be controlled through reducing chemical reactions between the particulates and the liquid. As a convenient method to fabricate Al-based composites, powder metallurgy is considered a superior method because it enables easier control of the interfacial layer. It also features other advan-

tages such as easy adjustment of the ingredients, the ability to produce homogeneous microstructures and clean interfaces, and convenient near-net shaping [4–6].

To avoid the aforementioned brittleness, particulates with metal characteristics can be used as reinforcement; such particulates will result in decreased brittleness of the bonding layer between particulates and the Al matrix. Recently, metallic particulates such as Ni, Fe, and Ti have been added to Al matrixes to form Ni$_x$Al$_y$, Al$_5$Fe$_2$, and Al$_3$Ti as intermetallic reinforcements in PRAMCs through *in situ* reaction [7–10]. The results show that the mechanical properties of the composites were improved. Because Al$_3$Ti exhibits a low density, a high modulus, good wear resistance, excellent specific strength, and a coefficient of thermal expansion similar to that of the Al matrix, it has attracted attention as a potential reinforcement material for Al-based composites [11–12]. Al$_3$Ti is attractive as a component for PRAMCs used in aviation, aerospace, and automotive applications. However, the literature contains few detailed studies of the microstructure development of Al$_3$Ti-containing PRAMCs during sintering and the effect of Al$_3$Ti on the mechanical properties of the

🖄 Springer

1432

Int. J. Miner. Metall. Mater., Vol. 24, No. 12, Dec. 2017

resultant composites.

In this work, an Al-based composite was prepared through powder metallurgy and subsequent extrusion. The metallic powder Ti was chosen as the original particles to form the core–shell-structured Al_3Ti reinforcement phase. The microstructure development and mechanical properties were then investigated. The mechanism of the formation of the core–shell structure is discussed. The results serve to improve the mechanical performance of Al-based composites.

2. Experimental

Gas-atomized pure Ti powder with particle diameters ranging from 30 to 50 μm and pure Al powder with an average particle diameter of (2 ± 0.5) μm were chosen as the starting materials. The micrographic morphologies of the two powders were observed under a Zeiss Sigma field-emission scanning electron microscope, as shown in Figs. 1(a) and 1(b). They were mixed with a mass ratio of 30:70 (the volume fraction of Ti particles was approximately 20%) in a planetary-type grinding machine. To obtain different interfacial bonding layers, the fully mixed powders were sintered at 600, 620, or 640°C under a reduced pressure of 4.0×10^{-3} Pa or less or under an elevated pressure of 150 MPa for 5 h. The sintering temperatures were selected on the bases of the work of Chianeh *et al.* [13] and the Al–Ti binary phase diagram [14]. Compared with the microstructures of the samples sintered at 600 and 640°C, the interfacial microstructure between the particles and the matrix of the sample sintered at 620°C was found to be superior. Thus, in subsequent experiments, the sample sintered at 620°C was chosen for extrusion at a mass ratio of 12.75:1 and 550°C.

The microstructures of the composites were observed under an Olympus GX71 optical microscope. The composition distribution of the interfacial microstructure was analyzed using a Zeiss Sigma scanning electron microscope equipped with an Oxford Instruments X-MAX20 energy-dispersive spectrometer. The texture of the extruded sample was measured using an Oxford Instruments Nordlys Nano electron backscattered diffractometer. The mechanical properties were tested at ambient temperature on an MTS Landmark electrohydraulic servo machine, and the fracture morphologies of the specimens were observed by scanning electron microscopy (SEM).
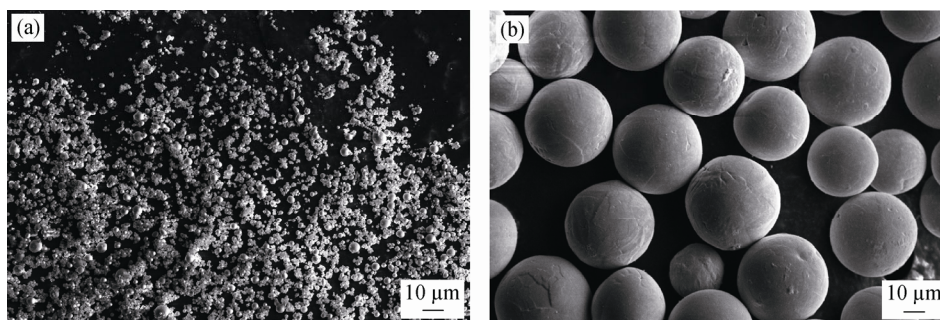

Fig. 1.   SEM micrographs of the Al powder (a) and the Ti powder (b) used as starting materials.

3. Results and discussion

3.1. Microstructure evolution during sintering

Fig. 2 shows the microstructures of the samples sintered at 600, 620, or 640°C for 5 h. Figs. 2(a) and 2(b) show that spherical Ti particles transformed into core–shell structures in the Al matrix. The average thickness of the transient layers between spherical Ti particles and the Al matrix was approximately 3–5 μm and 10–15 μm, respectively, which demonstrates that the thickness of the transient layer varied with the sintering temperature. When the sintering temperature was increased to 640°C (Fig. 2(c)), most of the core–shell-structured particles disappeared because of the complete diffusional phase transformation throughout the whole Ti particle body. These observations suggest that the shell thickness increased with increasing sintering temperature and that higher temperatures promoted diffusion and phase formation between the coupled metals.

The compositional distribution of a typical particle was analyzed by EDS by line scanning and point gauging, as shown in Fig. 3. The results illustrate that the content of Ti increased dramatically to the maximum level at the interface between the Ti particles and the Al matrix, whereas the Al content decreased. Thereafter, the Al content decreased to a low level, whereas the Ti content increased to a high level and fluctuated in a certain range (as shown in Fig. 3(b)). These results indicate that Al–Ti intermetallics formed from the interface to the edge of the remaining Ti core along the checking line and that the Ti near the center was almost unaffected by the diffusion reaction.
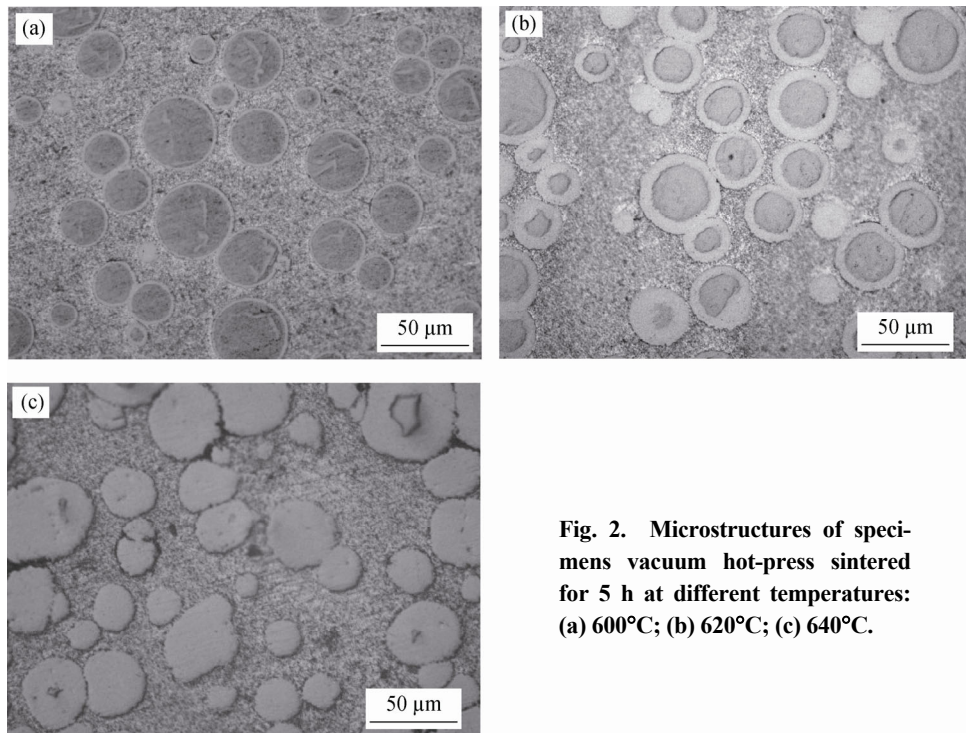
Fig. 2. Microstructures of specimens vacuum hot-press sintered for 5 h at different temperatures: (a) 600°C; (b) 620°C; (c) 640°C.
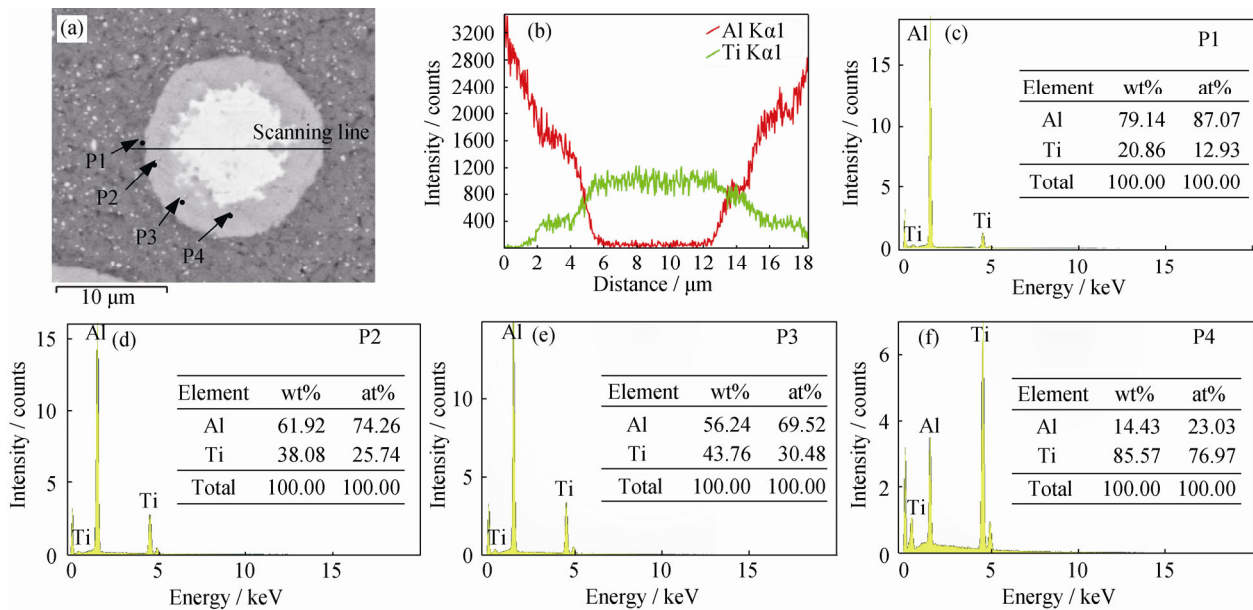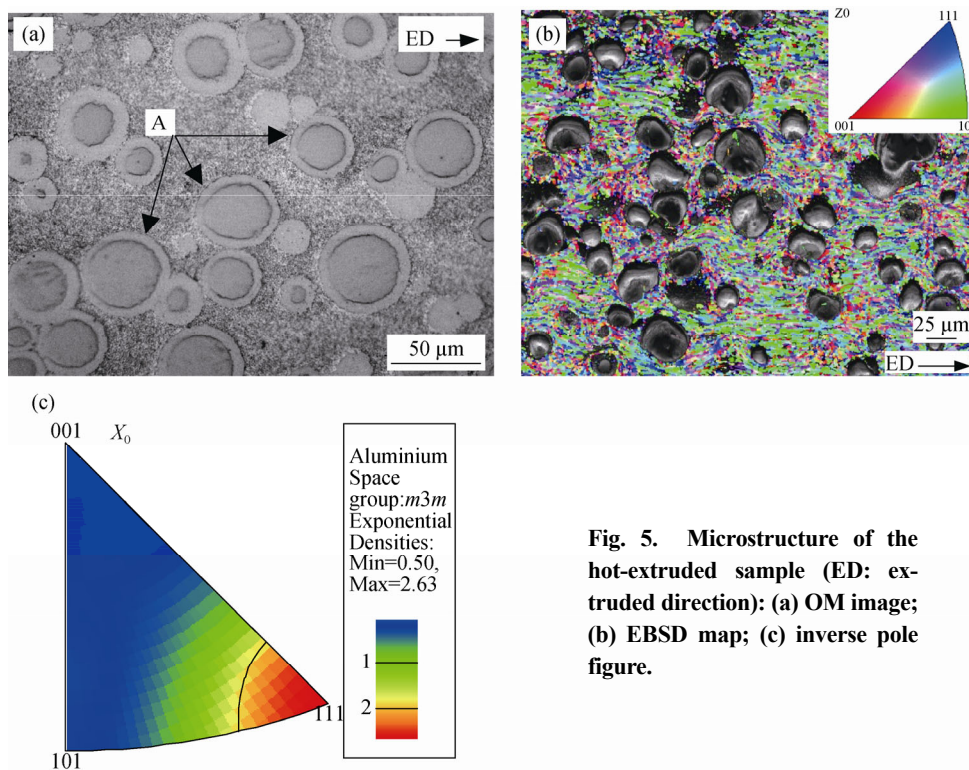

Fig. 3. EDS analysis of a typical reinforcement: (a) position of the analyses; (b) EDS line-scan spectrum; (c) spectrum of point P1; (d) spectrum of point P2; (e) spectrum of point P3; (f) spectrum of point P4.

The spectrum of typical points and the atomic ratio of Al/Ti at each point are shown in Fig. 3. The atomic ratio of Al/Ti decreased from P1 (Al-rich zone) to P4 (Ti-rich zone). The Al/Ti ratios at points P1, P2, P3, and P4 were 87.07:12.93, 74.26:25.74, 69.52:30.48, and 23.03:76.97, respectively (see Figs. 3(c)–3(f)). According to the atomic ratio of Al/Ti at point P1, some α-Al (i.e., a solid solution of Ti dissolved in Al) formed near the interface between the Al matrix and the original Ti powder. The atomic ratio of Al/Ti at point P2 is consistent with that of Al_3Ti, which means that the Al_3Ti intermetallic layers formed near the Al-rich zone. By contrast, the atomic ratio of Al/Ti at point P4 is consistent with that of Ti_3Al near the Ti-rich zone. The atomic ratio of Al/Ti decreases from the Al-rich zone to the Ti-rich zone along the formed intermetallic layer.

The XRD pattern (Fig. 4) indicates that α-Al, Al_3Ti, $AlTi_3$, and Ti phases co-exist in the core–shell-structured reinforced composite fabricated at 620°C for 5 h. These results dif-

1434

Int. J. Miner. Metall. Mater., Vol. 24, No. 12, Dec. 2017

fer somewhat from those reported previously. Liu *et al.* [15] observed that Al_3Ti was usually the unique phase in the Al/Ti interface for solid diffusion at 500–600°C; they deduced that Al_3Ti was the prevalent phase. However, Kerr *et al.* [16] demonstrated that $TiAl_2$ has a lower free energy than the other compounds in the Al–Ti system. Although trace amounts of $AlTi_3$ are present according to the peak intensity in the corresponding XRD pattern, the pattern also shows that both Al_3Ti and $AlTi_3$ formed through the diffusion reaction between the Al matrix and the original Ti particles. Al_3Ti is the preferential phase in the Al–Ti system because its free energy of formation is lower than that of $AlTi_3$ and AlTi [17]. Thus, $AlTi_3$ is a transient phase that should appear under certain conditions near the Ti-rich zone. These results are consistent with the transitional region between the α-Ti and Al_3Ti regions observed by Guo *et al.* [18] by high-resolution TEM (HRTEM). These results thus explain the formation of the transitional region in detail. By contrast, Guo *et al.* elsewhere reported that no other Al–Ti intermetallic phase existed between the α-Al and Al_3Ti regions [19]. The Ti that remains in the center as the plastic component of the reinforcement can reduce the crack sensitivity of reinforcements.

Fig. 4. XRD pattern of the Al–30Ti hot-press sintered at 620°C for 5 h.

3.2. Microstructure after hot extrusion

The selected sample was sintered at 620°C for 5 h to investigate its microstructure evolution after hot extrusion. The core–shell-structured Ti particles were stretched slightly along the extruded direction (see the particles marked with "A" in Fig. 5(a)) with no breakage of the core-shell-structured reinforcements; the Al matrix was subjected to the most severe plastic deformation during extrusion.

Fig. 5. Microstructure of the hot-extruded sample (ED: extruded direction): (a) OM image; (b) EBSD map; (c) inverse pole figure.

This configuration is well observed in both the EBSD mapping and the inverse pole figure (Figs. 5(b) and 5(c)). Very fine A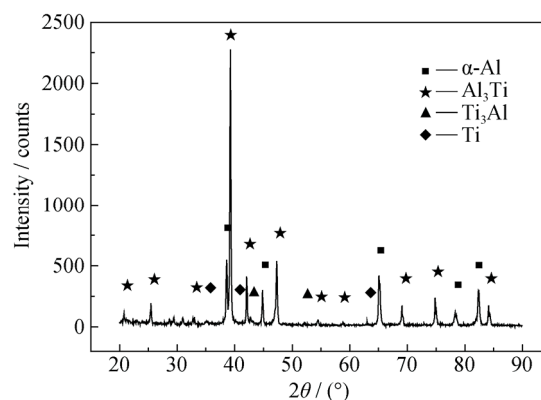l matrix grains with an average size of no less than 10 μm were formed along the extruded direction, and a distinct <111> fiber texture was developed after hot extrusion. The maximum level of the pole concentration was 2.63.

In general, the texture shows the anisotropy of the metal matrix composite (MMC) materials and affects the mechanical properties correspondingly.

3.3. Mechanical properties

The tensile specimens are cylindrical, with a diameter of $\phi 10$ mm at a gauge length of 30 mm. The compression specimens are cylindrical, with a diameter of $\phi 8$ mm at a gauge length of 8.5 mm. Both specimens were taken parallel to the extruded direction from the hot-extruded Al–Ti composites. The compression and tensile properties were tested at ambient temperature on an MTS Landmark hydraulic servo testing machine using an initial strain rate of 1×10^{-3}. The typical strain–stress curves of the tested sample are shown in Fig. 6. The yield strength (YS), ultimate tensile strength (UTS), and the elongation are 285 MPa, 304 MPa, and 14%, respectively. The compressed specimen became a small disk with a dimension of $\phi 13.6$ mm $\times$ 2.9 mm and no evident macrocracks, as shown in Fig. 7. The compression YS was as high as 280 MPa, whereas the deformation reached 60%. These promising mechanical properties of the composite are attributed to its special macro plasticity–hard-plasticity structure composed of the plastic Al matrix and the core–shell-structured Ti/Al$_3$Ti reinforcements. The Al/Al$_3$Ti interface, which exhibits lower interfacial energy, forms a strong bonding interface [20] and can contribute to such su-

perior mechanical behaviors of the composite. The strong interfacial bonding between Al$_3$Ti and the Al matrix is attributed to the crystal structures of Al$_3$Ti and Al because the tetragonal unit cell of Al$_3$Ti ($a = 0.3848$ nm and $c = 0.8596$ nm) is comparable to that of α-Al ($a = 0.4049$ nm) [19]. Under uniaxial tension or compression, the <111> texture would be favorable for strength because the {111} slip plane would be parallel to the tension or compression axis. In this case, the Schmid factor is zero. However, because the intensity of the fiber texture is weak and because aluminum has an FCC crystal microstructure, the influence of the texture on the mechanical properties of the composite should be limited.
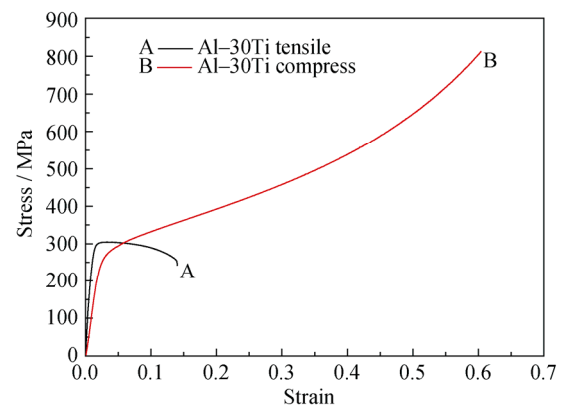

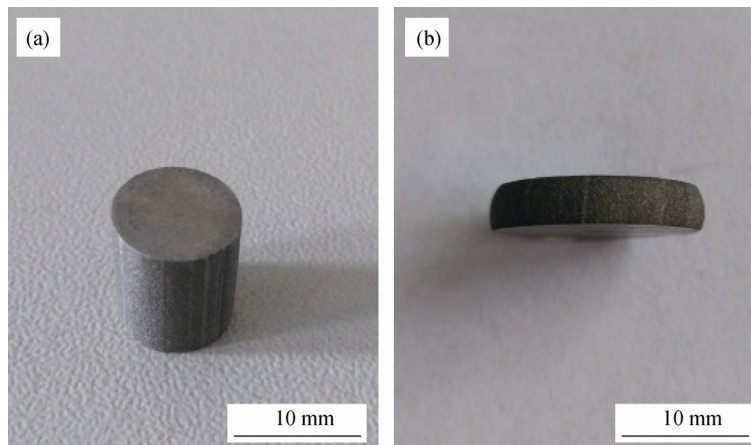**Fig. 6.   Typical engineering strain–stress curves of as-extruded specimens.**

Fig. 7.   Images of the compression specimen before (a) and after (b) compression.

Some fractured reinforcements surrounded by Al-matrix dimple morphology are observed in the typical fracture morphology of the tensile specimen (Fig. 8). These fractured reinforcements indicate that the Al–Ti intermetallic layer is still prone to failure, as observed at the positions marked A and B. However, the crack propagation can be pinned by the plastic Al matrix. Obvious tearing ridges are observed in the

Al matrix surrounding the reinforcements; these ridges contribute to the plasticity of this composite. Numerous small dimples in the Al matrix bond strongly with the reinforcement material. The superior mechanical performance of this composite is related to the strength of the Al–Ti intermetallics formed through interdiffusion and to good bonding between the reinforcements and the Al matrix. Another factor

improving the mechanical performance is the high plasticity of Ti metal particulates that remain in the center of the spherical reinforcements and the Al matrix. They enhance the plastic strain accommodation and reduce the crack sensitivity of the Al–Ti intermetallics at the interface between the Al matrix and spherical Ti reinforcement particles. Furthermore, the sharply refined grains formed during the hot-extrusion process can play an effective role in improving the properties of the composite.
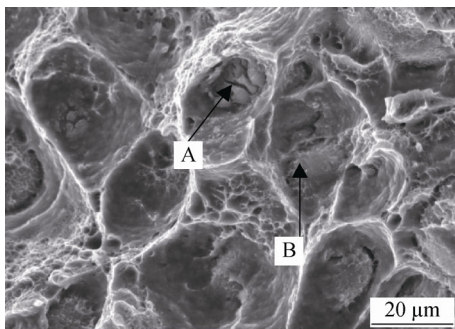

Fig. 8.   Typical fracture morphology of the Al–Ti composite after tensile testing.

4. Conclusions

A promising Al-matrix composite with core–shell- structured Ti/Al$_3$Ti reinforcements was fabricated through hot-press sintering followed by hot extrusion. After extrusion, the core–shell-structured reinforcements were observed to bond strongly with the Al matrix without breaking. The UTS and elongation reached 304 MPa and 14%, respectively, and the compress deformation reached 60%. The Al–Ti intermetallics, including the Al$_3$Ti phase, are the main part of the reinforcements; the remaining Ti core can play a reinforcement role and reduce the crack sensitivity of Al–Ti intermetallics. The mechanical properties were improved by controlling the relative thickness of the Al–Ti intermetallics and the inner Ti. The results demonstrate that the proposed approach is a promising method for fabricating high-performance composites through solid-state interdiffusion using a desirable metal powder as the starting reinforcement material.

Acknowledgements

References

[1]   X.Y. Liu, X.W. Lv, C.X. Li, and C.G. Bai, Wettability of Ti–Al alloys on TiN substrate at 1758 K, *Mater. Today Proc.*, 2(2015), p. S274.

[2]   D. Wearing, A.P. Horsfield, W. Xu, and P.D. Lee, Which wets TiB$_2$ inoculant particles: Al or Al$_3$Ti?, *J. Alloys Compd.*, 664(2015), p. 460.

[3]   X.M. Wang, A. Jha, and R. Brydson, *In situ* fabrication of Al$_3$Ti particle reinforced aluminium alloy metal–matrix composites, *Mater. Sci. Eng. A*, 364(2004), No. 1-2, p. 339.

[4]   J.M. Kunze and C.C. Bampton, Challenges to developing and producing MMCs for space applications, *JOM*, 53(2001), No. 4, p. 22.

[5]   E. Evangelista and S. Spigarelli, Constitutive equations for creep and plasticity of aluminum alloys produced by powder metallurgy and aluminum-based metal matrix composites, *Metall. Mater. Trans. A*, 33(2002), No. 2, p. 373.

[6]   J. Qin, G. Chen, C.H. Ji, X.G. Song, N. Hu, F. Han, and Z.M. Du, Effect of reaction temperature on the microstructures and mechanical properties of high-intensity ultrasonic assisted *in-situ* Al$_3$Ti/2024 Al composites, *J. Alloys Compd.*, 666(2016), p. 58.

[7]   W. Wu, B. Guo, Y. Xue, R. Shen, S. Ni, and M. Song, Ni-Al$_x$Ni$_y$ core–shell structured particle reinforced Al-based composites fabricated by *in-situ* powder metallurgy technique, *Mater. Chem. Phys.*, 160(2015), p. 352.

[8]   Y.C. Wang, M. Song, S. Ni, and Y. Xue, *In situ* formed core–shell structured particle reinforced aluminum matrix composites, *Mater. Des.*, 56(2014), No. 4, p. 405.

[9]   Y. Xue, R.J. Shen, S. Ni, M. Song, and D.H. Xiao, Fabrication, microstructure and mechanical properties of Al–Fe intermetallic particle reinforced Al-based composites, *J. Alloys Compd.*, 618(2015), p. 537.

[10] Y. Xue, R.J. Shen, S. Ni, D.H. Xiao, and M. Song, Effects of sintering atmosphere on the mechanical properties of Al–Fe particle-reinforced Al-based composites, *J. Mater. Eng. Perform.*, 24(2015), No. 5, p. 1890.

[11] D.J. Harach and K.S. Vecchio, Microstructure evolution in metal-intermetallic laminate (MIL) composites synthesized by reactive foil sintering in air, *Metall. Mater. Trans. A*, 32(2001), No. 6, p. 1493.

[12] E.B. Tochaee, H.R.M. Hosseini, and S.M.S. Reihani, Fabrication of high strength *in-situ* Al–Al$_3$Ti nanocomposite by mechanical alloying and hot extrusion: Investigation of fracture toughness, *Mater. Sci. Eng. A*, 658(2016), p. 246.

[13] V.A. Chianeh, H.R.M. Hosseini, and M. Nofa, Microstruc-

tural features and mechanical properties of Al−Al₃Ti composite fabricated by *in-situ* powder metallurgy route, *J. Alloys Compd.*, 473(2009), No. 1-2, p. 127.

[14] V. Raghavan, Al−Ti (Aluminum−Titanium), *J. Phase Equilib. Diffus.*, 26(2005), No. 2, p. 171.

[15] J.P. Liu, Y.Q. Su, Y.J. Xu, L.S. Luo, J.J. Guo, and H.Z. Fu, First phase selection in solid Ti/Al diffusion couple, *Rare Met. Mater. Eng.*, 40(2011), No. 5, p. 753.

[16] H.W. Kerr, J. Cisse, and G.F. Bolling, On equilibrium and non-equilibrium peritectic transformations, *Acta Metall.*, 22(1974), No. 6, p. 677.

[17] I. Ohnuma, Y. Fujita, H. Mitsui, K. Ishikawa, R. Kainuma, and K. Ishida, Phase equilibria in the Ti−Al binary system,

Acta Mater., 48(2000), No. 12, p. 3113.

[18] B. Guo, J.H. Yi, S. Ni, R.J. Shen, and M. Song, Factors affecting the microstructure and mechanical properties of Ti−Al₃Ti core−shell-structured particle-reinforced al matrix composites, *Philos. Mag.*, 96(2016), No. 12, p. 1197.

[19] B.S. Guo, S. Ni, R.J. Shen, and M. Song, Fabrication of Ti−Al₃Ti core−shell structured particle reinforced Al based composite with promising mechanical properties, *Mater. Sci. Eng. A*, 639(2015), p. 269.

[20] L. Zhang, B.L. Wu, Y.H. Zhao, and X.H. Du, Exploration of Al-based matrix composites reinforced by hierarchically spherical agents, *Int. J. Miner. Metall. Mater.*, 20(2013), No. 8, p. 796.